

Nanomechanical-resonator-assisted induced transparency in a Cooper-pair-box system

Xiao-Zhong Yuan,^{1,2} Hsi-Sheng Goan,^{1,3,*} Chien-Hung Lin,¹ Ka-Di Zhu,² and Yi-Wen Jiang²

¹*Department of Physics and Center for Theoretical Sciences,
National Taiwan University, Taipei 10617, Taiwan*

²*Department of Physics, Shanghai Jiao Tong University, Shanghai 200240, China*

³*Center for Quantum Science and Engineering, National Taiwan University, Taipei 10617, Taiwan*

We propose a scheme to demonstrate the electromagnetically induced transparency (EIT) in a system of a superconducting Cooper-pair box coupled to a nanomechanical resonator. In this scheme, the nanomechanical resonator plays an important role to contribute additional auxiliary energy levels to the Cooper-pair box so that the EIT phenomenon could be realized in such a system. We call it here resonator-assisted induced transparency (RAIT). This RAIT technique provides a detection scheme in a real experiment to measure physical properties, such as the vibration frequency and the decay rate, of the coupled nanomechanical resonator.

PACS numbers: 85.85.+j, 85.25.-j, 42.50.Gy

I. INTRODUCTION

To be able to observe quantum phenomena in mesoscopic (macroscopic) physical systems which contain many millions of atoms is of great importance in quantum mechanics and also quantum information science. Currently, there are experimental and theoretical groups devoting to observing quantum effects in truly solid-state mechanical oscillator or cantilever systems [1, 2, 3, 4, 5, 6, 7, 8, 9, 10, 11, 12, 13, 14, 15, 16, 17, 18, 19, 20, 21, 22]. In the regime when the individual mechanical quanta are of the order or greater than the thermal energy, quantum effects become important and the motion of the mechanical resonator or cantilever is close to or on the verge of the quantum limit. Coupling such a mechanical system to an electrical motional transducer might enable us to observe and control the motional quantum state of the mechanical system.

A Superconducting Cooper-pair box (CPB) [23, 24, 25, 26, 27, 28] consists of a superconducting island (box) weakly linking to a superconducting reservoir by a Josephson tunnel junction. The coherent controls and manipulations of the effective two-level quantum system of a CPB (a charge qubit) have been demonstrated [23, 25, 26]. Due to its controllability, a CPB has been proposed to be one of ideal candidates to act as a transducer or a mediator to couple to a nanomechanical resonator (NR). With appropriate quantum state controls of a CPB, the CPB has been proposed to be used to produce desired NR Fock state and perform a quantum non-demolition (QND) measurement of NR Fock state [29], to drive a NR into a superposition of spatially separated states and probe their decoherence rate [30], to cool the NR to its ground state and generate squeezed state of the NR [31], to probe the quantum mechanical feature of tiny motions of a NR [32], to integrate a superconducting transmission line resonator with a NR [33], and to demonstrate progressive quantum decoherence [34].

Recently, a high-frequency mechanical resonator beam that operates in the GHz range has been reported [35]. For a NR operating at the fundamental frequency of GHz and at a temperature of 10-100mK, some interesting phenomena close to or on the verge of the quantum limit may be observed. In this paper, we propose a scheme to demonstrate the electromagnetically induced transparency (EIT) in a system of a superconducting CPB qubit coupled to a NR. The conventional EIT effect occurs in an ensemble of three-level Λ -type atomic system with two lower states coupled respectively to an excited state with two laser fields (control and probe fields) [36, 37]. A typical experiment is conducted by scanning the probe laser frequency and measuring its transmitted intensity. The transparency of the medium takes place when the absorption on both transitions is suppressed due to destructive interference between excitation pathways to the common upper level. In addition to the absorption eliminated via quantum interference, the EIT effect has also been shown to be an active mechanism to slow down or stop light pulse completely in various systems, such as ultracold gas of sodium atoms [38], rare-earth-ion-doped crystals [39], semiconductor quantum wells [40], quantum dot exciton systems [41], and systems with four-level or multi-level cells [42]. Recently, it has been proposed to use a superconductive analogy to EIT in a persistent-current flux qubit biased in a Λ configuration to probe small qubit errors due to decoherence or imperfect state preparation [43, 44]. Here we show that the EIT phenomenon could be realized in an effective two-level superconducting CPB charge qubit coupled to a NR. The

*Electronic address: goan@phys.ntu.edu.tw

capacitive CPB-NR coupling plays an important role to contribute additional auxiliary energy levels for EIT to occur. As a result, this resonator-assisted induced transparency (RAIT) technique provides a detection scheme in a real experiment to measure physical properties, such as the vibration frequency and the decay rate of the coupled NR, or the decay and decoherence rates of the CPB qubit, if one set of the values of either the CPB or the NR properties is known by other means.

II. MODEL AND CALCULATIONS

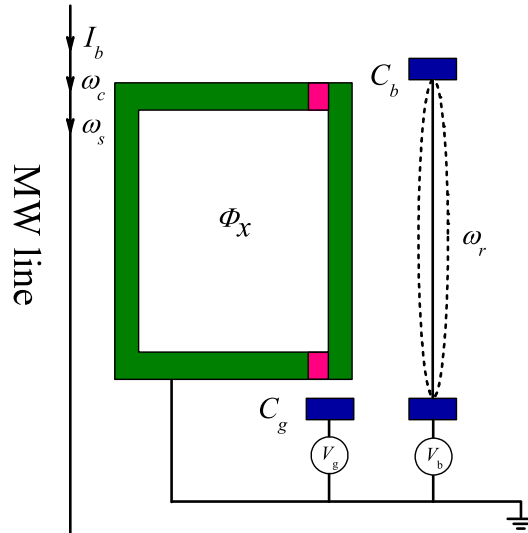


FIG. 1: Schematic diagram of a nanomechanical resonator (NR) coupled to a Cooper-pair box (CPB) qubit. The microwave currents (with frequencies ω_s , ω_c) and a direct current (I_b) are applied to flow along the MW line beside the CPB to control the magnetic flux through the CPB loop.

In our model, we assume that a nanomechanical-resonator (NR) couples capacitively to a Cooper-pair box (CPB) qubit (see Fig. 1). The tunnel junction of the CPB shown in Fig. 1 is split into two to form a SQUID loop [23, 25] which allows us to control its effective Josephson energy with a small external magnetic field or magnetic flux. Two microwave currents are applied in a microwave (MW) line [45] beside the CPB to induce oscillating magnetic fields in the Josephson junction SQUID loop of the CPB qubit. We call one of them the control current with frequency ω_c and amplitude \mathcal{E}_c . The other is called the signal (probe) current with frequency ω_s and amplitude \mathcal{E}_s . In addition, a direct current I_b is also applied to the MW line to control the magnetic flux through the SQUID loop and thus the effective Josephson coupling of the CPB qubit. The Hamiltonian of the total system can be written as [29, 33]:

$$H = H_{CPB} + H_{NR} + H_{int}, \quad (1)$$

$$H_{CPB} = \hbar\omega_q S_z - \hbar E_J \cos \left[\frac{\pi\phi_x(t)}{\phi_0} \right] S_x, \quad (2)$$

$$H_{NR} = \hbar\omega_r a^\dagger a, \quad (3)$$

$$H_{int} = 2\hbar\lambda(a^\dagger + a)S_z. \quad (4)$$

Here H_{CPB} and H_{NR} are respectively the Hamiltonians of the CPB qubit and the NR. H_{int} is the interaction between them [29]. The operators a , a^\dagger denote the creation and annihilation operators for the NR with frequency ω_r and mass m . The two-level system of the CPB qubit can be characterized by the pseudospin-1/2 operators S_z and $S_x = S_+ + S_-$. $\omega_q = 4E_C(2n_g - 1)$ is the electrostatic energy and E_J is the maximum Josephson energy. Here, $E_C = e^2/(2C_\Sigma)$ is the charging energy with C_Σ the total CPB capacitance and $n_g = (C_b V_b + C_g V_g)/(2e)$ is the dimensionless gate charge, where C_g and V_g are, respectively, the gate capacitance and gate voltage of the CPB qubit, and C_b and V_b are, respectively, the capacitance and voltage between the NR and the CPB island. The capacitive interaction strength can be written as $\lambda = 4E_C C_g V_g / (2de\sqrt{2\hbar m\omega_r})$, where d is the distance between the NR and the CPB [29]. The coupling between the MW line and the CPB qubit in the second term of Eq. (2) results from the total externally applied magnetic flux $\phi_x(t) = \phi_q(t) + \phi_b$ through the CPB qubit loop of an effective area S with $\phi_0 = \hbar/(2e)$ being the flux quantum [33]. Here

$$\phi_q(t) = \mu_0 S I(t)/(2\pi r), \quad (5)$$

with r being the distance between the MW line and the qubit, and μ_0 being the vacuum permeability [33]. $\phi_q(t)$ and ϕ_b are produced, respectively, by the microwave current

$$I(t) = \mathcal{E}_c \cos(\omega_c t) + \mathcal{E}_s \cos(\omega_s t + \delta') \quad (6)$$

and the direct current I_b in the MW line. For simplicity, we assume the phase factor $\delta' = 0$ as it is not difficult to show that the results of this paper do not depend on the value of δ' .

Choosing the direct current I_b and the microwave current $I(t)$ such that $\phi_b \gg \phi_q(t)$ and $\pi\phi_b/\phi_0 = \pi/2$, we have

$$\hbar E_J \cos\left[\frac{\pi\phi_x(t)}{\phi_0}\right] \approx -\hbar E_J \frac{\pi\phi_q(t)}{\phi_0}. \quad (7)$$

We can work in a frame rotating at the frequency ω_c of the control current and the total Hamiltonian in this rotating frame becomes

$$\begin{aligned} H_c = & \hbar\Delta S_z + \hbar\omega_r a^\dagger a + 2\hbar\lambda(a^\dagger + a)S_z \\ & + \hbar\Omega(S_+ + S_-) + \mu\mathcal{E}_s(S_+ e^{-i\delta t} + S_- e^{i\delta t}). \end{aligned} \quad (8)$$

In analogy to the case of a two-level atom driven by bichromatic electromagnetic waves, here

$$\mu = \mu_0 S \hbar E_J / (4r\phi_0) \quad (9)$$

is the effective ‘‘electric dipole moment’’ of the qubit,

$$\Omega = \mu\mathcal{E}_c/\hbar \quad (10)$$

is the effective ‘‘Rabi frequency’’ through the control current,

$$\Delta = \omega_q - \omega_c \quad (11)$$

is the detuning between the CPB qubit resonance frequency and control current frequency, and

$$\delta = \omega_s - \omega_c \quad (12)$$

is the detuning between the signal (probe) current frequency and the control current frequency.

Furthermore, we may take into account the decoherence and relaxation of the CPB qubit and NR by including their coupling to external environments into the Hamiltonian [46, 47, 48, 49]. We assume that the environments to which the CPB and NR couple respectively could be described as independent ensembles of harmonic oscillators with respective spectral densities characterizing their properties. We also assume that the NR interacts bilinearly with the environment through their position operators, and the CPB interacts through S_x operator and S_z operator with the environment position operators. The S_x coupling to the environment models the relaxation (and thus also decoherence) process of the CPB qubit, while the S_z coupling to the environment models the pure dephasing process of the CPB qubit [46, 47, 48, 49]. Generally speaking, the value of ω_q of the CPB qubit is considerably greater than the value of ω_r of the NR. Therefore, it may be plausible to apply the rotating-wave approximation to the CPB-environment coupling term, but not for NR-environment coupling term in the system-environment interaction Hamiltonian. By following the standard procedure [46, 47, 48, 49], it is then straightforward to derive the Born-Markovian master equation of the reduced density matrix of the CPB-NR system, $\rho(t)$, through tracing out the environmental degrees of freedom as:

$$\begin{aligned} \frac{d\rho}{dt} = & -\frac{i}{\hbar} [H_c, \rho] + A \{[S_-, [S_+, \rho]] + h.c.\} + B \{[S_-, \{S_+, \rho\}] + h.c.\} \\ & + E [S_z, [S_z, \rho]] + D [Q, [Q, \rho]] + G [Q, [P, \rho]] + \frac{i}{\hbar} L [Q, \{P, \rho\}], \end{aligned} \quad (13)$$

where $Q = -2\lambda(a^\dagger + a)$ and P are the position and momentum operators of the NR, respectively. The coefficients A, B, E, D, G and L are related to the characteristics of the coupling, and to the structure and properties of the environments. Their explicit forms can be written as

$$A = -\frac{1}{2\hbar} \left\{ \frac{\gamma_1}{2} (1 + 2N(\omega_q)) \right\}, \quad (14)$$

$$B = \frac{1}{2\hbar} \left\{ \frac{\gamma_1}{2} \right\}, \quad (15)$$

$$E = -\frac{1}{\hbar} \left\{ \frac{\gamma_2}{2} (1 + 2N(0)) \right\}, \quad (16)$$

$$D = -\frac{1}{4\hbar} \gamma_3 (1 + 2N(\omega_r)), \quad (17)$$

$$G = -\frac{1}{2\hbar} \frac{1}{m\omega_r} \Delta_3, \quad (18)$$

$$L = -\frac{1}{4m\omega_r} \gamma_3, \quad (19)$$

where

$$\gamma_1 = 2\pi J_x(\omega_q), \quad (20)$$

$$\gamma_2 = 2\pi J_z(0), \quad (21)$$

$$\gamma_3 = 2\pi J_R(\omega_r), \quad (22)$$

$$\Delta_3 = \mathcal{P} \int_0^\infty d\omega \frac{J_R(\omega)}{\omega - \omega_r} (1 + 2N(\omega)). \quad (23)$$

Here, J_x , J_z and J_R are the spectral densities of the respective environments coupled through S_x and S_z to the CPB, and through Q to the NR, respectively. $N(\omega) = 1/[\exp(\hbar\omega/k_B T) - 1]$ is the Boltzman-Einstein distribution of the thermal equilibrium environments. \mathcal{P} denotes the principal value of the argument. Note that ω_r and ω_q in H_c in Eq. (13) should be regarded as the real physical frequencies in which the renormalization and Lamb shifts due to the interactions with the environments have been included. With the master equation (13), we can obtain the equation of motion for the mean (or expectation value) of any physical operation O of the CPB-NR system by calculating $\langle \dot{O}(t) \rangle = Tr[O\dot{\rho}(t)]$. For convenience, in the following we denote variable $O(t)$ as its expectation value $\langle O(t) \rangle$, and will clarify its definition when there is a potential confusion. We thus have

$$\frac{dS_-}{dt} = \left[-\frac{1}{T_2} - i(\Delta + Q) \right] S_- + 2i\Omega S_z + 2\frac{i}{\hbar} \mu S_z \mathcal{E}_s e^{-i\delta t}, \quad (24)$$

$$\frac{dS_z}{dt} = -\frac{1}{T_1} \left(S_z + \frac{1}{2} \right) - i\Omega(S_+ - S_-) - i\frac{\mu}{\hbar} (S_+ \mathcal{E}_s e^{-i\delta t} - S_- \mathcal{E}_s^* e^{i\delta t}), \quad (25)$$

$$\frac{d^2 Q}{dt^2} + \gamma \frac{dQ}{dt} + \omega_r^2 Q = -8\omega_r^3 \lambda_0 S_z, \quad (26)$$

where

$$\lambda_0 = \lambda^2 / \omega_r^2. \quad (27)$$

Please note that the variables S_- , S_z and Q in Eqs. (24)-(26) stand for the expectation values of their corresponding operators, respectively, except that the product of the variables Q and S_- in Eq. (24) should be regarded as $\langle Q S_- \rangle$. The decoherence time T_2 and excited-state relaxation time T_1 of the CPB qubit, and the decay rate γ of the NR are derived microscopically as

$$T_2 = \left[\frac{1}{\hbar} \left\{ \frac{\gamma_1}{2} (1 + 2N(\omega_q)) \right\} + \frac{4}{\hbar} \left\{ \frac{\gamma_2}{2} (1 + 2N(0)) \right\} \right]^{-1}, \quad (28)$$

$$T_1 = \left[\frac{2}{\hbar} \left\{ \frac{\gamma_1}{2} (1 + 2N(\omega_q)) \right\} \right]^{-1}, \quad (29)$$

$$\gamma = \frac{1}{2m\omega_r} \gamma_3. \quad (30)$$

Note that if the pure dephasing coupling were dropped, i.e., $\gamma_2 = 0$, then $T_2 = 2T_1$. This is often the case for a two-level atomic system. After defining $p = \mu S_-$, $k = 2S_z$, we have

$$\frac{dp}{dt} = \left[-\frac{1}{T_2} - i(\Delta + Q) \right] p + i\frac{\mu^2 k \mathcal{E}}{\hbar}, \quad (31)$$

$$\frac{dk}{dt} = -\frac{1}{T_1} (k + 1) - 4\frac{\text{Im}(p\mathcal{E}^*)}{\hbar}, \quad (32)$$

$$\frac{d^2 Q}{dt^2} + \gamma \frac{dQ}{dt} + \omega_r^2 Q = -4\lambda_0 \omega_r^3 k, \quad (33)$$

where $\mathcal{E} = \mathcal{E}_c + \mathcal{E}_s e^{-i\delta t}$ and $\mathcal{E}_c = \hbar\Omega/\mu$. Note that the Qp term in Eq. (31) should be regarded as the expectation value of $\langle Qp \rangle$. The above equations can not be solved as they are not closed.

In order to solve these equations, we first take the semiclassical approach by factorizing the NR and CPB qubit degrees of freedom, i.e., $\langle Qp \rangle = \langle Q \rangle \langle p \rangle$. This ignores any entanglement between these systems. We will study the EIT behavior in the context of a weak signal (probe) current amplitude \mathcal{E}_s in the presence of a strong control current amplitude \mathcal{E}_c . To obtain analytical solution, we make the ansatz

$$p = p_0 + p_1 e^{-i\delta t} + p_{-1} e^{i\delta t}, \quad (34)$$

$$k = k_0 + k_1 e^{-i\delta t} + k_{-1} e^{i\delta t}, \quad (35)$$

$$Q = Q_0 + Q_1 e^{-i\delta t} + Q_{-1} e^{i\delta t}. \quad (36)$$

By substituting Eqs. (34)-(36) into Eqs. (31)-(33) and working to the lowest order in \mathcal{E}_s , we finally obtain in the steady-state the following solutions

$$k_1 = \frac{2\frac{T_1}{T_2}\Omega_c^2 k_0 \theta}{\frac{T_1}{T_2}i\delta_0 - 1 - 2\frac{T_1}{T_2}\beta} \cdot \frac{\mathcal{E}_s}{\mathcal{E}_c}, \quad (37)$$

$$p_1 = \frac{\frac{i4\lambda_0 k_1 \omega_r^3}{-\delta^2 - i\gamma\delta + \omega_r^2} \cdot \frac{\mu^2 k_0 \mathcal{E}_c}{\Delta - 4\lambda_0 \omega_r k_0 - \frac{i}{T_2}} + i\mu^2(k_0 \mathcal{E}_s + k_1 \mathcal{E}_c)}{i\hbar(\Delta - 4\lambda_0 \omega_r k_0 - \delta) + \frac{\hbar}{T_2}}, \quad (38)$$

where

$$\theta = \frac{1}{i(\Delta_c - 4\lambda_0 \omega_0 k_0 - \delta_0) + 1} + \frac{i}{\Delta_c - 4\lambda_0 \omega_0 k_0 + i}, \quad (39)$$

$$\beta = \frac{4\lambda_0 \omega_r \eta \frac{\Omega_c^2 k_0}{\Delta_c - 4\lambda_0 \omega_0 k_0 - i} + \Omega_c^2}{i(\Delta_c - 4\lambda_0 \omega_0 k_0 - \delta_0) + 1} + \frac{4\lambda_0 \omega_0 \eta \frac{\Omega_c^2 k_0}{\Delta_c - 4\lambda_0 \omega_0 k_0 + i} + \Omega_c^2}{-i(\Delta_c - 4\lambda_0 \omega_0 k_0 + \delta_0) + 1}, \quad (40)$$

$$\eta = \frac{\omega_0^2}{\omega_0^2 - i\gamma_0 \delta_0 - \delta_0^2}, \quad (41)$$

and dimensionless variables $\omega_0 = \omega_r T_2$, $\gamma_0 = \gamma T_2$, $\delta_0 = \delta T_2$, $\Omega_c = \Omega T_2$, and $\Delta_c = \Delta T_2$ are introduced for later numerical convenience. The zero-order population inversion of the CPB is determined by the following equation:

$$(k_0 + 1)[(\Delta_c - 4\lambda_0 \omega_0 k_0)^2 + 1] + 4\frac{T_1}{T_2}\Omega_c^2 k_0 = 0. \quad (42)$$

The cubic Eq. (42) has either a single or three real roots. The latter case just corresponds to the intrinsic bistable states which we will not discuss here.

To observe the EIT phenomena, we calculate the absorption power of the signal (probe) current as a function of its frequency. We note that the second term containing S_x in Eq. (2) describing the Cooper-pair tunneling energy controlled by the external flux which is induced by the applied MW line current. By using the approximation of Eq. (7), the absorption power of the signal current can be expressed as

$$P_{abs} = \pi \frac{\hbar E_J}{\phi_0} S_x \frac{d\phi_s}{dt}, \quad (43)$$

where $\phi_s = \mu_0 S I_s / (2\pi r)$ is the magnetic flux produced by the signal current $I_s = \mathcal{E}_s \cos(\omega_s t)$. There are several terms in S_x as indicated in Eq. (34) which is written in the frame rotating at the control current frequency ω_c . It is obvious that only the terms $p_1 e^{-i\omega_s t}$ and $p_1^* e^{i\omega_s t}$ in the laboratory frame have non-zero contributions to the time-averaged absorption power which can be measured in experiments. In this way, after the time average, we have

$$P_{abs} = -2\mu \mathcal{E}_s \omega_s \text{Im}(p_1), \quad (44)$$

where Im denotes taking the imaginary part, and $\mu = \mu_0 S \hbar E_J / (4r\phi_0)$.

III. EXPERIMENTAL PARAMETERS AND RESULTS

We discuss how the EIT phenomena could be designed and realized in the CPB-NR system with realistically reasonable parameters. The typical values of the charging energy E_C and the Josephson coupling energy E_J of a

CPB charge qubit are often designed such that $E_C \gg E_J$, so $E_C = 40$ GHz and $E_J = 2$ GHz are chosen. The values $\lambda = 50$ MHz and $\omega_r = 1$ GHz are used as in Refs. [4, 29, 30, 32]. The decay (relaxation) rate and decoherence rate of the CPB system depend on temperatures and the qubit operational points which could be controlled by the external gate voltage and magnetic flux. It has been reported that the relaxation rate $1/T_1 = 4$ MHz [31, 50] and the decoherence time T_2 can reach the order of microsecond at the degeneracy point [51]. In our system, the CPB qubit may not be tuned at the degeneracy point, so it could be sensitive to the inevitable charge noise that is present in the circuits. Hence we choose the decoherence rate conservatively to be $1/T_2 = 20$ MHz. The dominant mechanism for the damping of the resonator mode may come from the coupling to the phonon modes of the support, which could lead to the decay rate $\gamma = 0.01$ MHz [31]. For numerical convenience, we use dimensionless quantities for these quantities as follows. $\gamma_0 = \gamma T_2 = 5 \times 10^{-4}$, $\omega_0 = \omega_r T_2 = 50$, $\lambda_0 = \lambda^2/\omega_r^2 = 2.5 \times 10^{-3}$. For $S = 1 \mu\text{m}^2$, $r = 1 \mu\text{m}$, and $\mathcal{E}_c = 200 \mu\text{A}$, we have $\mu/\hbar = \mu_0 S E_J / (4r\phi_0) \approx 300$ GHz/A, $\Omega_c = \Omega T_2 = (\mu/\hbar)\mathcal{E}_c T_2 = 3$.

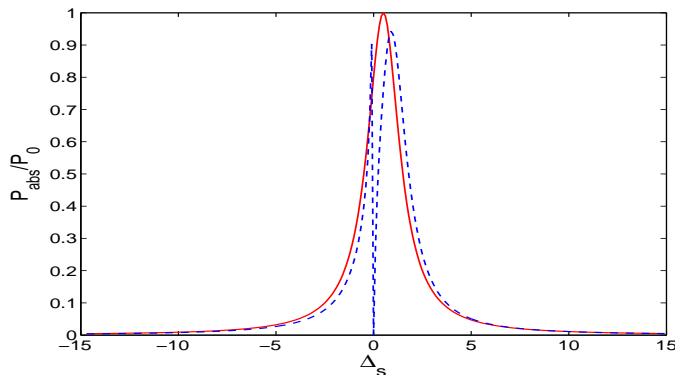


FIG. 2: Scaled absorption power profiles of the signal current as a function of the detuning Δ_s for $\Omega_c = 0$ (solid curve) and $\Omega_c = 3$ (dashed curve). Other parameters used are $\lambda_0 = 2.5 \times 10^{-3}$, $\Delta_c = \omega_0 = 50$, $\gamma_0 = 5 \times 10^{-4}$.

Figure 2 plots the absorption power of the signal current P_{abs} of Eq. (44) as a function of the detuning Δ_s ($\Delta_s = (\omega_s - \omega_q)T_2$). The absorption power is scaled in unit of P_0 which is the maximum value of P_{abs} when $\Omega_c = 0$. In the absent of the control current ($\Omega_c = 0$), the solid curve shows a standard resonance absorption profile of the signal current in the CPB system, with the centre of the curve shifted from the resonance $\omega_s = \omega_q$ a bit. This is due to the coupling λ_0 between the CPB and NR [29, 32]. Furthermore, the resonant frequency shift increases with the increase of the coupling constant λ_0 . When the control current is turned on ($\Omega_c = 3$), a narrow non-absorption hole appears at $\Delta_s = 0$ as shown in the dashed curve in Fig. 2. This indicates that the signal current has a narrow peak of induced transparency (no absorption). Without the coupling λ_0 between the CPB and NR, such a phenomenon will not appear. This can be seen from Fig. 3 in which a standard absorption resonance profile for $\lambda_0 = 0$ (in solid line) appears. The central resonance peak shifts also a little bit from $\Delta_s = 0$ (i.e., $\omega_s = \omega_q$) due to the presence of the control current ($\Omega_c = 3$). When $\lambda_0 \neq 0$ (dashed and dot-dashed curves), the coupling prevents absorption of the signal (probe) current in a narrow portion of the resonance profile. Therefore, we call it resonator-assisted induced transparency (RAIT). As we have chosen $\Delta_c = \omega_0$, the minima of the non-absorption holes (valleys) appear at $\Delta_s = 0$ in Fig. 2 and Fig. 3. Otherwise, they will move away from the point $\Delta_s = 0$. Recently, Radeonychev *et al.* [52] have shown that resonant transparency could occur in a two-level quantum system induced via mechanical (acoustical) harmonic vibration of a solid medium along the propagation of multi-frequency laser radiation. They concluded that the atomic acoustical vibration plays a key role in this so-called acoustically induced transparency (AIT).

Alternatively, we may also understand how the RAIT could occur in the CPB and NR system as follows. We first consider the NR and CPB system without the application of the control and signal MW currents. The Hamiltonian, excluding the coupling to the external environments, from Eq. (8) is then

$$H_c = \hbar\omega_q S_z + \hbar\omega_r a^\dagger a + 2\hbar\lambda(a^\dagger + a)S_z. \quad (45)$$

The capacitive coupling between the CPB and the NR indicates that one charge state of the CPB will attract the NR and shift its equilibrium position near the CPB, while the other charge state will repel the CPB. Therefore, a displaced oscillator basis will allow us to use the ordinary harmonic oscillator formalism within each displaced potential well. The Hamiltonian of Eq. (45) can then be diagonalized [53, 54] in the eigenbasis of

$$|\pm, N_\pm\rangle = |\pm\rangle_z \otimes e^{\mp(\lambda/\omega_r)(a^\dagger - a)}|N\rangle, \quad (46)$$

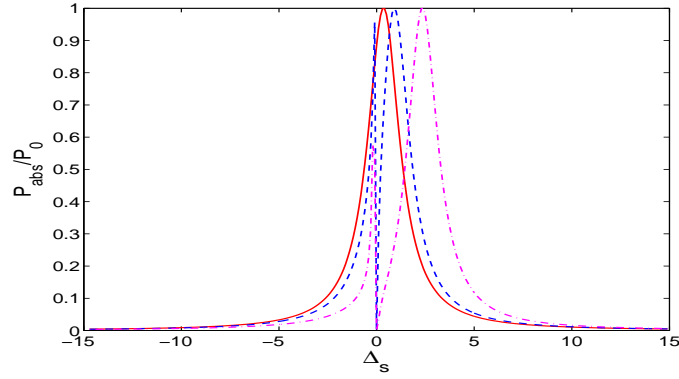


FIG. 3: Shifts of the absorption resonance profiles for different values of the coupling constant λ_0 between the CPB and NR: $\lambda_0 = 0$ (solid curve), $\lambda_0 = 2.5 \times 10^{-3}$ (dashed curve), and $\lambda_0 = 0.01$ (dot-dashed curve). Other parameters used are $\Omega_c = 3$, $\Delta_c = \omega_0 = 50$, $\gamma_0 = 5 \times 10^{-4}$.

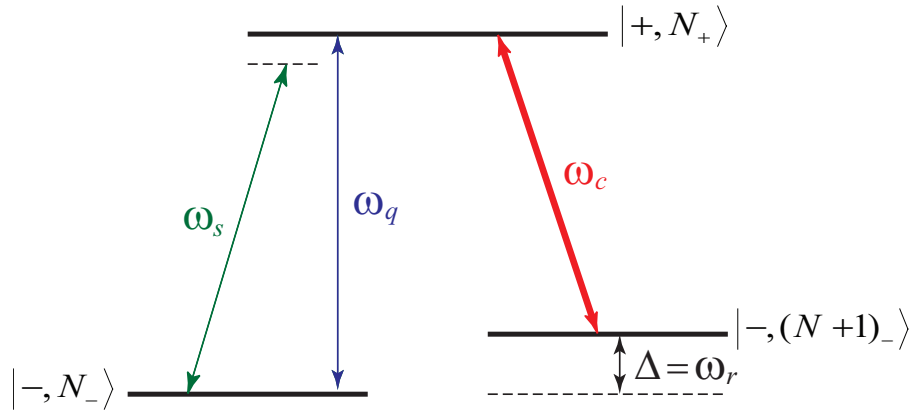


FIG. 4: Schematic illustration of quantum three-level structure in the coupled CPB-NR system. Here a strong control current of frequency ω_c is tuned on resonance between the $|+, N_+\rangle$ and $|-, (N+1)_-\rangle$ transition with $\Delta = \omega_q - \omega_c = \omega_r$, where ω_r is the resonant frequency of the NR and ω_q is the resonant frequency of the CPB qubit. A weak signal (probe) current with a tunable frequency ω_s is applied, and its absorption power profile near the resonant frequency of the CPB qubit is measured.

with the eigenenergies

$$E_{\pm} = \pm \hbar \omega_q + \hbar \omega_r (N - \lambda_0), \quad (47)$$

where the CPB qubit states $|\pm\rangle_z$ are eigenstates of S_z with the excited state $|+\rangle_z = |e\rangle$ and the ground state $|-\rangle_z = |g\rangle$, the oscillator states $|N_{\pm}\rangle$ are position-displaced Fock states, and λ_0 is defined in Eq. (27). Note that $|+, N_+\rangle$ and $|-, N_-\rangle$ form, respectively, an orthonormal basis with $\langle M_+ | N_+ \rangle = \delta_{MN}$ and $\langle M_- | N_- \rangle = \delta_{MN}$, but the states $|N_+\rangle$ and $|N_-\rangle$ are not mutually orthogonal and their inner products are given by [53, 54]

$$\langle M_- | N_+ \rangle = e^{-2\lambda_0} \left(\frac{2\lambda}{\omega_r} \right)^{N-M} \sqrt{\frac{M!}{N!}} L_M^{N-M}(4\lambda_0), \quad (48)$$

where $L_k^j(y)$ is the associated Laguerre polynomial. Thus the coupling to NR could provide the CPB qubit with additional auxiliary energy levels to realize the EIT phenomena. For the parameters used in the simulations, the quantum three levels that may realize the EIT phenomena could be chosen as $|-, N_-\rangle$, $|-, (N+1)_-\rangle$ and $|+, N_+\rangle$ illustrated in Fig. 4. In Fig. 4, the state $|-, N_-\rangle$ has the same parity as state $|-, (N+1)_-\rangle$, and thus the effective electric-dipole transition is forbidden. On the other hand, the state $|+, N_+\rangle$ is of opposite parity and thus has a non-zero effective electric-dipole coupling to both $|-, N_-\rangle$ and $|-, (N+1)_-\rangle$ states. These conditions satisfy the specific restrictions on the configuration of the three levels (states) in atoms to realize EIT. That is, two of the three possible transitions between the states must be dipole-allowed, i.e. the transitions can be induced by an oscillating

electric field. The third transition should be dipole-forbidden. In our setup, the strong control field (current) is tuned on resonance between the $|+, N_+\rangle$ and $|-, (N+1)_-\rangle$ transition. The weak probe or signal current is tuned near resonance between the two states, $|+, N_+\rangle$ and $|-, N_-\rangle$. Then the signal-current absorption power profile of the transition is measured. As in a conventional three-level Λ -type atomic system [36, 37], the strong control field current with the detuning equal to the vibration frequency of the NR drives the coupled CPB-NR system. As a result, the dressed CPB-NR coupled system becomes transparent for a weak signal current with a frequency matching the resonant frequency of CPB qubit. We note that the selection rule here is somewhat different from that of the superconducting flux-qubit circuit which shows a EIT phenomenon in a Λ configuration [43, 44]. There, dipole-like coupling is allowed between all pairs of levels due to the symmetry breaking of the potential of the flux qubit [55].

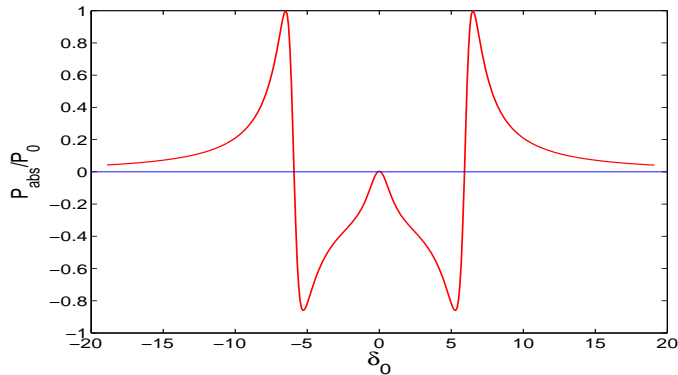


FIG. 5: Signal current absorption profile for $\lambda_0 = 0$ (no interaction between CPB and NR), $\Delta_c = 0$ (driven exactly on resonance) and $\Omega_c = 3$ (by a strong control field). The negative values of the absorption profile represent stimulated emission, i.e., amplification of the signal current. Other parameters used are $\gamma_0 = 5 \times 10^{-4}$, and $(T_2/T_1) = 0.2$.

Note that the decay rates of levels $|+, N_+\rangle$ are much larger than those of levels $|-, N_-\rangle$ for arbitrary values of N although they have roughly the same decoherence rates. This is because $|-\rangle_z = |g\rangle$ is assumed to be the lowest electronic energy state of the CPB qubit and the phonon number decay rate γ is taken to be much smaller than T_1^{-1} and T_2^{-1} ($\gamma T_2 = \gamma_0 = 5 \times 10^{-4}$, and $T_2/T_1 = 0.2$). Due to these decay and decoherence rates, the condition [37] for which all the important features of the RAIT remains considerably observable requires $\Omega^2 \gg (T_1 T_2)^{-1}$ or equivalently $\Omega_c^2 \gg (T_2/T_1)$. For the parameters chosen in Figs. 2 and 3 for our CPB-NR system, the condition is well satisfied. If, however, the value of ω_c decreases and the value of the ratio (T_2/T_1) increases, then the EIT absorption hole (dip) will become shallow. In a two-level atomic system driven by a strong, resonant field, when the Rabi frequency of the driving field is greater than the atomic decay rate, the resonance fluorescence spectrum exhibits three-peak structure, called Mollow three-peak spectrum [56, 57]. If we set $\lambda_0 = 0$ (no interaction between the CPB qubit and the NR) and $\Delta_c = 0$ (i.e., the control current resonantly interacting with the CPB qubit) with Ω_c much larger than the decay rate of the CPB qubit, a Mollow three-peak spectrum but with different relative peak widths compared to a two-level atomic system could be expected in our CPB qubit system. The difference in the peak widths lies on the fact that usually $T_2/T_1 = 2$ in an atomic system [see Eqs. (28) and (29) if the pure dephasing rate $\gamma_2 = 0$], while a typical value of $T_2/T_1 = 0.2$ is chosen for the CPB qubit system. If we apply a weak probe field (signal current) and calculate the signal-current absorption power profile, we find that the signal-current absorption power profile takes on the negative values (see Fig. 5), representing stimulated emission rather than absorption [58, 59]. This amplification of the signal current may be understood to happen primarily at the expense of the strong driving (control) current, which experiences an increased attenuation rate. Similar amplification of the probe-field profile in a strongly driven two-level atomic system at optical frequencies was predicted in Ref. [58] and experimentally observed and verified in Ref. [59].

The essential point of RAIT in our system is that the absorption power of the signal current goes abruptly to zero (almost) for $\omega_s = \omega_c + \omega_r$. This gives us a method to measure the vibration frequency of the NR with high precision. The procedure is as follows. Fixing the frequency of the control current which is close to the resonant frequency of the CPB, and changing the frequency of the signal current, when the signal current becomes transparent, obviously we have $\omega_s = \omega_c + \omega_r$, i.e., the difference between the frequency of the control current and the signal current is the frequency of the NR, ω_r . One can also see from Fig. 3 that the width of the absorption hole (valley) increases with the increasing values of λ_0 . This can be understood as follows. With the increase of the coupling strength λ_0 , the absorption peak shifts to the right, and the minima of the non-absorption hole (valley) appears however at $\Delta_s = 0$ (as we have chosen $\Delta_c = \omega_0$ mentioned above). As a result, the width of the absorption hole (valley) increases.

In Fig. 6, we draw the absorption power as a function of the NR decay rate γ_0 for $\Delta_s = 0$. Again, the absorption power is scaled in unit of P_0 which is the maximum value of P for the parameters chosen in Fig. 6. It shows that the absorption power of the signal current increases with the increase of the decay rate of the NR. In this way, we can determine the decay rate of the NR and investigate its relation with the environmental temperatures according to the absorption power of the signal current.

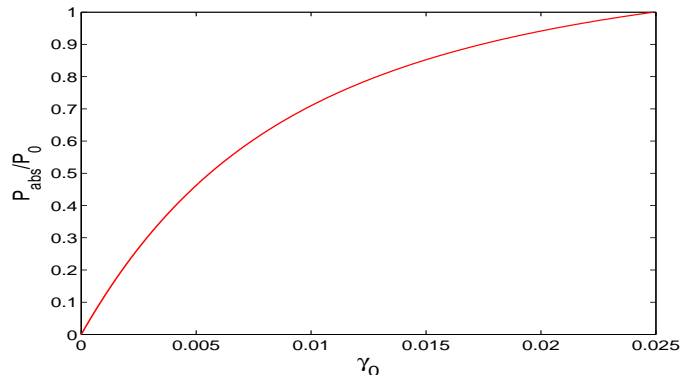


FIG. 6: Scaled absorption power of the signal current as a function of the NR decay rate γ_0 for $\Delta_s = 0$. Other parameters used are $\Omega_c = 3$, $\lambda_0 = 2.5 \times 10^{-3}$, and $\Delta_c = \omega_0 = 50$.

IV. CONCLUSION

In conclusion, we have demonstrated the EIT phenomena in a system of a CPB qubit coupled to a NR. Though the CPB is an effective two-level system, the NR contributes additional auxiliary energy levels so that the EIT phenomena can be realized in such a system. Without the NR, the EIT phenomena will disappear. So we call our scheme resonator-assisted induced transparency (RAIT). Our proposal which is within the reach of current experimental technology provides a detection scheme to measure physical properties, such as the vibration frequency and the decay rate of the coupled NR, or the decay and decoherence rates of the CPB qubit, if one set of the values of either the CPB or NR properties is known by other means. We have specifically demonstrated here a case to measure the vibration frequency and the decay rate of the NR using the RAIT technique. Such a high contrast and high accuracy NR frequency measurement could potentially provide an alternative way to other NR measurement schemes, such as magnetomotive detection.

Acknowledgments

This work has been supported in part by the National Natural Science Foundation of China and the National Minister of Education Program for Changjiang Scholars and Innovative Research Team in University (PCSIRT). HSG would like to acknowledge support from the National Science Council, Taiwan under grant numbers NSC96-2112-M-002-007 and NSC97-2112-M-002-012-MY3, support from the National Taiwan University, Taiwan under grant number 97R0066-67, and support from the focus group program of the National Center for Theoretical Sciences, Taiwan. XZY acknowledges support from the National Natural Science Foundation of China under grant number 10874117. KDZ acknowledges support from the National Natural Science Foundation of China under grant number 10774101.

-
- [1] M. F. Bocko and R. Onofrio, *Rev. Mod. Phys.* **68**, 755 (1996).
- [2] M. Roukes, *Phys. World* **14**:2, 25 FEB (2001); H. G. Craighead, *Science* **290**, 1532 (2000).
- [3] M. Blencowe, *Phys. Rep.* **395**, 159 (2004).
- [4] K. C. Schwab and L. C. Roukes, *Phys. Today*, July 36 (2005).
- [5] R. G. Knobel and A. N. Cleland, *Nature (London)* **424**, 291 (2003).
- [6] M. D. LaHaye, O. Buu, B. Camarota and K. C. Schwab, *Science* **304**, 74 (2004).
- [7] A. Naik, O. Buu, M. D. LaHaye, A. D. Armour, A. A. Clerk, M. P. Blencowe and K. C. Schwab, *Nature* **443**, 193 (2006).
- [8] W. Marshall, C. Simon, R. Penrose and D. Bouwmeester, *Phys. Rev. Lett.* **91**, 130401 (2003).
- [9] S. Mancini, V. Giovannetti, D. Vitali and P. Tombesi, *Phys. Rev. Lett.* **88**, 120401 (2002).
- [10] D. H. Santamore, H.-S. Goan, G. J. Milburn and M. L. Roukes, *Phys. Rev. A* **70**, 052105 (2004).
- [11] W. K. Hensinger, D. W. Utami, H.-S. Goan, K. Schwab, C. Monroe and G. J. Milburn, *Phys. Rev. A* **72**, 041405(R) (2005).
- [12] S. Bose et al., *New J. Phys.* **8**, 34 (2006).
- [13] V. Peano et al., *New J. Phys.* **8**, 21 (2006).
- [14] S. Pirandola, D. Vitali, P. Tombesi and S. Lloyd, *Phys. Rev. Lett.* **97**, 150403 (2006).
- [15] F. Xue, Y.-X. Liu, C. P. Sun and F. Nori, *Phys. Rev. B* **76**, 064305 (2007).
- [16] K. Audenaert, J. Eisert, M. B. Plenio and R. F. Werner, *Phys. Rev. A* **66**, 042327 (2002).
- [17] M. B. Plenio, J. Hartley, and J. Eisert, *New J. Phys.* **6**, 36 (2004).
- [18] J. Eisert, M. B. Plenio, S. Bose, and J. Hartley, *Phys. Rev. Lett.* **93**, 190402 (2004).
- [19] K.-L. Liu and H.-S. Goan, *Phys. Rev. A* **76**, 022312 (2007).
- [20] K. Jacobs, P. Lougovski and M. Blencowe, *Phys. Rev. Lett.* **98**, 147201 (2007).
- [21] A. A. Clerk and D. W. Utami, *Phys. Rev. A* **75**, 042302 (2007).
- [22] E. Buks et al., *Europhys. Lett.* **81**, 10001 (2008).
- [23] Y. Nakamura, Yu. A. Pashkin and J. S. Tsai, *Nature* **398**, 786 (1999).
- [24] Y. Makhlin G. Schön, and A. Shnirman, *Rev. Mod. Phys.* **73**, 357 (2001).
- [25] O. Astafiev, Y. A. Pashkin, Y. Nakamura, T. Yamamoto, and J. S. Tsai, *Phys. Rev. Lett.* **93**, 267007 (2004).
- [26] T. Duty , D. Gunnarsson, K. Bladh, and P. Delsing, *Phys. Rev. B* **69**, 140503(R) (2004).
- [27] J.Q. You and F. Nori, *Phys. Today* **58**, No. 11, 42 (2005).
- [28] J. Clarke and F. K. Wilhelm, *Nature* **453**, 1031 (2008).
- [29] E. K. Irish and K. Schwab, *Phys. Rev. B* **68**, 155311 (2003).
- [30] A. D. Armour, M. P. Blencowe, and K. C. Schwab, *Phys. Rev. Lett.* **88**, 148301 (2002).
- [31] I. Martin, A. Shnirman, L. Tian and P. Zoller, *Phys. Rev. B* **69**, 125339 (2004); I. Rabl, A. Shnirman and P. Zoller, *Phys. Rev. B* **70**, 205304 (2004).
- [32] L. F. Wei, Y. X. Liu, C. P. Sun and Franco Nori, *Phys. Rev. Lett.* **97**, 237201 (2006).
- [33] C. P. Sun, L. F. Wei, Y. X. Liu and Franco Nori, *Phys. Rev. A* **73**, 022318 (2006).
- [34] Y. D. Wang, Y. B. Gao and C. P. Sun, *Eur. Phys. J. B* **40**, 321 (2004).
- [35] X. M. H. Huang, C. A. Zorman, M. Mehregany and M. L. Roukes, *Nature (London)* **421**, 496 (2003).
- [36] S. E. Harris, *Phys. Today* **50** (7), 36 (1997).
- [37] M. Fleischhauer, A. Imamoglu and J. P. Marangos, *Rev. Mod. Phys.* **77**, 633 (2005).
- [38] L. V. Hau, S. E. Harris, Z. Dutton and C. H. Behroozi, *Nature* **379**, 594 (1999).
- [39] B. S. Ham, P. R. Hemmer, M. S. Shahriar, *Opt. Commun.* **144**, 227, (1997).
- [40] G. B. Serapiglia, E. Paspalakis, C. Sirtori, K. L. Vodopyanov and C. C. Phillips, *Phys. Rev. Lett.* **84**, 1019 (2000).
- [41] Y. W. Jiang, K. D. Zhu, Z. J. Wu, X. Z. Yuan and M. Yao, *J. Phys. B* **39**, 2621 (2006).
- [42] E. Paspalakis and P. L. Knight, *Phys. Rev. A* **66**, 015802 (2002).
- [43] K. V. R. M. Murali, Z. Dutton, W. D. Oliver, D. S. Crankshaw and T. P. Orlando, *Phys. Rev. Lett.* **93**, 087003 (2004).
- [44] Z. Dutton, K. V. R. M. Murali, W. D. Oliver and T. P. Orlando, *Phys. Rev. B* **73**, 104516 (2006).
- [45] I. Chiorescu, Y. Nakamura, C. J. P. M. Harmans, and J. E. Mooij, *Science* **299**, 1869 (2003).
- [46] C. W. Gardiner and P. Zoller, *Quantum Noise*, 2nd ed. (Springer, Berlin, 2000).
- [47] D.F. Walls and G.J. Milburn, *Quantum Optics* (Springer Study Edition, Berlin, 1994)
- [48] H. Carmichael, *Statistical Methods in Quantum Optics I* (Springer, Berlin, 1999).
- [49] H.-P. Breuer and F. Petruccione, *The Theory of Open Quantum Systems* (Oxford University Press, Oxford, 2002).
- [50] K. W. Lehnert, K. Bladh, L. F. Spietz, D. Gunnarsson, D. I. Schuster, P. Delsing, and R. J. Schoelkopf, *Phys. Rev. Lett.* **90**, 027002 (2003).
- [51] D. Vion, A. Aassime, A. Cottet, P. Joyez, H. Pothier, C. Urbina, D. Esteve and M. H. Devoret, *Science* **296**, 886 (2002); Y. Yu, S. Han, X. Chu, S. I. Chu and Z. Wang, *Science* **296**, 889 (2002).
- [52] Y.V. Radeonychev, M.D. Tokman, A.G. Litvak, and Olga Kocharovskaya, *Phys. Rev. Lett.* **96**, 093602 (2006).
- [53] E. K. Irish, J. Gea-Banacloche, I. Martin and K. C. Schwab, *Phys. Rev. B* **72**, 195410 (2005).
- [54] E. K. Irish, *Phys. Rev. Lett.* **99**, 173601 (2007).
- [55] Y. X. Liu, J. Q. You, L. F. Wei, C. P. Sun and F. Nori, *Phys. Rev. Lett.* **95**, 087001 (2005).
- [56] B.R. Mollow, *Phys. Rev.* **188**, 1969 (1969); *Phys. Rev. A* **2**, 76 (1970).
- [57] M. O. Scully and M. S. Zubairy, *Quantum Optics* (Cambridge University Press, Cambridge, 1997).

- [58] B.R. Mollow, Phys. Rev. A **5**, 2217 (1972).
- [59] F.Y. Wu, S. Ezekiel, M. Ducloy, B.R. Mollow, Phys. Rev. Lett. **38**, 19 (1977).